ELSEVIER

Journal of Hazardous Materials A95 (2002) 13–25

Journal of Hazardous Materials

www.elsevier.com/locate/jhazmat

# Effect of air in the thermal decomposition of 50 mass% hydroxylamine/water

Lizbeth O. Cisneros, William J. Rogers, M.S. Mannan*

*Mary Kay O'Connor Process Safety Center, Chemical Engineering Department, Texas A&M University, College Station, TX 77843-3122, USA*

Received 25 January 2002; received in revised form 10 June 2002; accepted 11 June 2002

**Abstract**

This paper presents experimental measurements of 50 mass% hydroxylamine (HA)/water thermal decomposition in air and vacuum environments using an automatic pressure tracking adiabatic calorimeter (APTAC). Overall kinetics, onset temperatures, non-condensable pressures, times to maximum rate, heat and pressure rates versus temperature, and mixture vapor pressures for the experiments in vacuum were similar when compared to the corresponding data for HA decomposition in air. Determined was an overall activation energy of 119 ± 8 kJ/mol (29 ± 2 kcal/mol), which is low compared to 257 kJ/mol (61.3 kcal/mol) required to break the $H_2N$–OH bond reported in the literature. The availability of oxygen from air did not affect detected runaway decomposition products, which were $H_2$, $N_2$, $N_2O$, NO, and $NH_3$, for samples run in vacuum or with air above the sample. A $\Delta H_{rxn}$ of −117 kJ/mol (28 kcal/mol) was estimated for the HA decomposition reaction under runaway conditions.


*Keywords:* Hydroxylamine; Thermal decomposition in vacuum; Kinetics; APTAC; Decomposition products

## 1. Introduction

The Mary Kay O'Connor Process Safety Center is studying 50 mass% hydroxylamine (HA)/water, which has important industrial uses. This concentration was selected for measurement because it is the highest available for industrial purposes. In spite of its importance, there is limited information about HA thermal behavior [1–3], and HA has been involved in two recent incidents causing the death of nine people [2,3]. The focus of the research reported here is the difference in thermal behavior for the decomposition of HA with air and

* Corresponding author. Tel.: +1-979-845-3489; fax: +1-979-458-1493.
*E-mail address:* mannan@tamu.edu (M.S. Mannan).

0304-3894/02/$ – see front matter © 2002 Elsevier Science B.V. All rights reserved.
PII: S0304-3894(02)00163-2

without air (vacuum). These measurements are needed, because a difference in thermal behavior detected between the two environments will directly affect process safety strategies for handling of hydroxylamine solutions. These results also will help to elucidate possible mechanisms for HA decomposition by demonstrating whether external oxygen from air participates significantly in the reaction.

## 2. Background

The thermal decomposition products of HA are not completely known. Some well-recognized process safety handbooks such as Sax's *Dangerous Properties of Industrial Materials* report the decomposition products to include $NO_x$ gases. A possible overall reaction for the formation of these products is the following:

$$3NH_2OH_{(liq)} \rightarrow NO_{(gas)} + NO_{2(gas)} + NH_{3(gas)} + 3H_{2(gas)} \quad (1)$$

Due to the scarcity of heat of formation data for hydroxylamine, calculation of $\Delta H_{rxn}$ for this reaction is uncertain. Reported values for the standard heat of formation of hydroxylamine liquid vary from −90.8 kJ/mol (−21.7 kcal/mol) [4] to −106.7 kJ/mol (−25.5 kcal/mol) [5] for a $\Delta H_{rxn}$ for Eq. (1) between 117 and 133 kJ/mol (28 and 32 kcal/mol). These values are endothermic contrary to our experimental observations of exothermic HA decomposition. Therefore, Eq. (1) is not dominant in the overall decomposition reaction. The following reaction is suggested by [4]:

$$2NH_2OH_{(gas)} + 0.5O_2 \rightarrow 3H_2O_{(gas)} + N_2 \quad (2)$$

This reference also mentions that Eq. (2) yields an estimated heat release of −248 kJ/mol (−59.2 kcal/mol). This value differs from the −320 kJ/mol (−76.5 kcal/mol) obtained when a $\Delta_f H^\circ$ $NH_2OH_{(gas)}$ of −10.2 kcal/mol as reported in [6] is used. If Eq. (2) is important in the overall decomposition reaction of HA, at least some of the experimental measurements (onset temperature, non-condensable pressure, time to maximum rate, heat and pressure rate versus temperature, and vapor pressure of the mixture) for samples run with air should differ from those of the samples run in vacuum.

Additional references describe the complex nature of the HA decomposition reaction system by addressing the possibility of distinct pathways depending on the pH [7]:

$$3NH_2OH \rightarrow NH_3 + N_2 + 3H_2O \quad \text{(in alkaline solutions)} \quad (3)$$

$$4NH_2OH \rightarrow N_2O + 2NH_3 + 3H_2O \quad \text{(in acid solutions)} \quad (4)$$

Both of these reactions are exothermic. Because HA samples are alkaline (pH >10), Eq. (3) could be considered the predominant reaction during the thermal runaway of HA. This hypothesis is proven wrong when compared to the experimental values presented in this paper.

There are qualitative reports of HA decomposition products under a variety of conditions. The species NO, $N_2O$, $N_2$, and $NH_3$ have been detected when hydroxylamine decomposes over Nuchar© in refluxing isopropanol [8]. $N_2O$ and $NH_4^+$ were detected when HA disproportionates in acid media [9]. Lunak and Veprek-Siska [10] stated that the decomposition

products of HA in alkaline media are $NH_3$, $N_2$, $N_2O$, and hyponitrite ($N_2O_2^{2-}$) and assumed that the reaction proceeds through the nitroxyl (HNO) intermediate. Lunak confirmed the presence of intermediates $N_2$ and $N_2O$ when the decomposition reactions were carried out under certain conditions and with various metal catalysts. It was assumed by Lunak that HA decomposition does not occur without a metal catalyst.

For process safety, it is important to determine the decomposition products under runaway conditions, which are similar to the conditions in the event of a process upset. HA decomposition products under runaway conditions have not been measured and could be different than those mentioned earlier, mainly because of the following reasons.

1. The liberated self-heat significantly increases the temperature, which can activate a wider spectrum of reactions.
2. Because the experiments are carried out in a closed cell environment, all of the decomposition products and reactants can react further.

## 3. Experimental details

### *3.1. Samples*

To determine HA decomposition products under runaway conditions, we utilized a well-characterized sample from Aldrich (Aldrich Hydroxylamine 99.999% 50 mass% solution in water, no. 46,780-4). Industrial HA samples contain unidentified proprietary stabilizers and therefore were not used for these studies.

### *3.2. Apparatus*

Data were collected using an automatic pressure tracking adiabatic calorimeter (APTAC), which is discussed elsewhere [11]. During a run, the pressure outside the sample cell is controlled with nitrogen to match the pressure inside the sample cell. This feature allows the use of relatively thin sample cells with low thermal inertia. This feature also facilitates the use of cell materials that cannot withstand a relatively high pressure differential such as glass. Several heating modes can be programmed in the APTAC such as heat-wait-search (HWS), isothermal, and temperature ramp. Among the recorded data are time, temperature, pressure, heat rate, and pressure rate. For the experiments reported here, the APTAC was modified to support a vacuum in the sample cell.

### *3.3. Analytical methods*

For the analytical measurements of the gas phase, a 3-Tesla Fourier Transform Mass Spectrometer (FTMS) also known as Ion Cyclotron Resonance Mass Spectrometry (ICR-MS) was used. The source was electron impact (EI) at 70 eV for 5 ms with scanning ranging from 11 to 10,000 *m*/*z* (mass to charge). The sample was introduced into the FTMS chamber until a pressure of 3.0E−8 Torr was achieved. Also, a gas chromatograph (GC) was used for product analysis.

Liquid products were analyzed for ammonia using a titration. Semi-quantitative energy disperse spectrums were run for some solid residues using a Cameka electron microscope. Atomic absorption (AA) proved the presence of a bluish ammonia–copper complex.

### 3.4. Experimental method

For the present work, all APTAC experiments were performed in a closed cell environment. Some experiments were run with ambient air above the sample, and for the others, the air was evacuated. The air evacuation procedure consisted of two parts.

1. HA samples (∼8 g) were transferred to glass sample cells using disposable plastic pipettes. Sample masses were obtained by weight differences. For the kinetic analysis, it was important to follow the exothermic behavior until completion, and the sample size used was the maximum possible under this restriction. Because of the relative small amounts of sample, no stirring was used during the APTAC runs.
2. The sample cell was mounted into the APTAC calorimeter. Liquid nitrogen was used to freeze the sample to −102 °C before removing air by vacuum (<0.5 psia) in one operation. For some samples this procedure was repeated up to three times with no difference in the results. After the air above the sample was removed, the valve that isolated the sample cell and sample transducer from the rest of the calorimeter was closed.

The heating mode was heat-wait-search in which the sample was heated to an initial search temperature of 50 °C and the temperature was allowed to stabilize (20 min). Then if exothermic activity was detected, as exhibited by a threshold temperature rise of 0.1 °C/min, the apparatus followed the reaction adiabatically until the reaction ended or until one of the pre-selected safety shutdown criteria was met. The APTAC can follow an exothermic reaction adiabatically for self-heating rates up to ∼400 °C/min. For the reported studies, the APTAC programmed shutdown criteria were: temperature, 460 °C; pressure, 10,342 kPa (1500 psia); temperature rate, 400 °C/min; and pressure rate, ∼68,900 kPa/min (10,000 psia/min). If no exothermic activity was detected within 20 min, the sample was heated to the next search temperature (10 °C higher) and the procedure was repeated until a preset maximum search temperature was attained (200 °C).

A sample thermocouple with a black Teflon-coated sheath (0.06 in. i.d.) was used to prevent the metal sheath from contacting the sample and catalyzing the HA decomposition [2]. Experimental runs were performed in borosilicate glass sample cells of 130 $cm^3$ nominal volume. It was presumed that glass cells provided a neutral environment without significant catalysis for the HA decomposition.

### 3.5. Uncertainties

A type-N thermocouple was used to measure sample temperatures with an overall absolute uncertainty of ∼±1 °C, and was checked periodically at 0 °C using an ice bath. Sensotec absolute pressure transducers with an overall uncertainty of ∼±42 kPa (∼6 psia) measured sample pressures and were checked frequently for agreement with ambient pressures. Sample masses were measured with a precision of ±0.01 g.

## 4. Results and discussion

### 4.1. Thermal behavior

Table 1 presents a summary of the experimental conditions along with the physical appearance of the sample residues after the experiments were completed and the samples returned to room temperature and exposed to air. No differences were observed in the physical aspects of the residue between samples run with air or in an evacuated environment. In all the experiments, the liquid residues were crystal clear when attached to the calorimeter, but some of the liquid samples turned blue when removed from the calorimeter.

Some of the liquid residue was put into an amber container to test the effect of light on the change in color, but this residue also turned blue. When the pH was changed from basic to acid, the blue color disappeared, but when the pH was set basic, again the color reappeared. That behavior was an indication of a possible complex formation. It is known that the copper(II) ion ammonia complex $Cu(NH_3)_4{}^{2+}$ has a deep blue color, and 165 ppm copper was measured in the liquid residue samples using atomic absorption. The probable source of the copper was the tube heater assembly of the APTAC.

Apart from the liquid residue, there was a thin layer of a white solid attached to the glass sample cell. This layer was not soluble in water, acid, or basic solutions and could not be removed. No solid residue was expected given the species involved in the reaction. The solid residue, tested using a Cameka electron microprobe, consisted mostly of Si. It is a well-documented fact that silica ($SiO_2$), the main component of the glass sample cells, has increased solubility as pH increases. A consistent explanation for the formation of this solid is that part of the glass sample cell dissolved at the high temperature generated during the runaway reaction and the high pH of the solution and then re-crystallized to form the white solid residue.

Table 1
Summary of HA decomposition data

| Run conditions | Sample identification | Mass ± 0.01 (g) | | Liquid residue | Solid residue |
|---|---|---|---|---|---|
| | | Initial | Final | | |
| Air | HA, air 1 | 8.09 | 3.13 | Bluish[a] | White |
| Air | HA, air 2 | 8.04 | 3.54 | Bluish[a] | White |
| Air | HA, air 3 | 8.03 | 5.15 | Clear | White |
| Air | HA, air 4 | 8.01 | 4.98 | Clear | White |
| Air | HA, air 5 | 8.02 | 3.90 | Clear | White |
| Air | HA, air 6 | 8.01 | 1.39 | Bluish[a] | White |
| Air | HA, air 7 | 8.00 | 2.66 | Clear | White |
| Vacuum | HA, vacuum 1 | 8.01 | 3.62 | Bluish[a] | White |
| Vacuum | HA, vacuum 2 | 8.03 | 3.08 | Bluish[a] | White |
| Vacuum | HA, vacuum 3 | 8.01 | 2.88 | Clear | White |
| Vacuum | HA, vacuum 4 | 8.01 | 4.12 | Clear | White |
| Vacuum | HA, vacuum 5 | 8.01 | 3.86 | Bluish[a] | White |
| Vacuum | HA, vacuum 6 | 8.02 | 3.20 | Clear | White |

[a] When exposed to air.

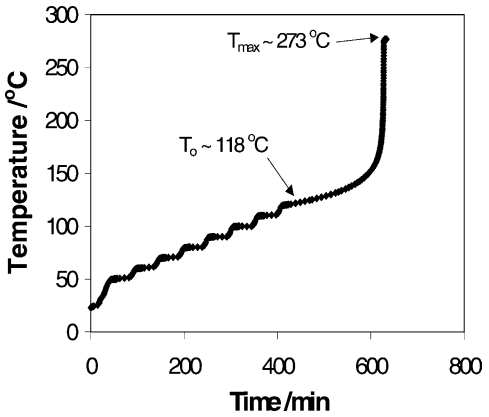


Fig. 1. Experimental temperature for HA decomposition in air (HWS mode, $\phi = 2$).

Fig. 1 presents a typical HWS routine for the performed experiments with and without air, where the exotherm is finished at $T_{max}$ ~273 °C. A summary of the data measured is presented in Table 2. The reported uncertainties are one standard deviation measured within the experimental replicas. The onset temperatures and the maximum adiabatic temperatures agree within experimental uncertainty for the experiments performed with and without air ($T_{on}$ = 117.5 and 118.5 °C; $T_{max}$ = 273 and 274 °C, respectively), which correspond to similar adiabatic temperature rises ($\Delta T_{adb}$) of 155 and 156 °C, respectively.

Because the samples run in vacuum start at a lower pressure, the maximum increase in pressure, $\Delta P_{max}$, (pressure at $T_{max}$ − pressure at $T_{on}$) is reported instead of the maximum pressure. The non-condensable pressure is the difference between the pressure after the experiment was completed and cooled to 50 °C and the pressure when the sample was first heated to 50 °C. The non-condensable pressure provides an estimate of the produced gas, which is not tempered by consumption of latent heat.

The time to maximum heat rate, $t_{MR,}$ estimates the available response time to prevent a possible runaway reaction. The time to maximum rate reported in Table 2 is the interval from the time that a self-heat rate of 0.1 °C/min was detected and the time that the maximum heat generation rate was observed. $\Delta P_{max}$, non-condensable pressure, and $t_{MR}$ reported in Table 2 in the two oxygen environments are equal within experimental error.

Some clues about the decomposition pathway are provided by the pressure data. Note that although the $\Delta P_{max}$ is high (6212 kPa (901 psia) in air and 6316 kPa (916 psia) in vacuum),

Table 2
Measured HA decomposition parameters

| Sample | Runs | $T_{on}$ (°C) | $T_{max}$ (°C) | $\Delta T_{adb}$ (°C) | $\Delta P_{max}$ (kPa) | Non-condensable pressure (kPa) | $t_{MR}$ (min) |
|---|---|---|---|---|---|---|---|
| HA, air | 7 | 117.5 ± 6 | 272.8 ± 5 | 155 ± 7 | 6212 ± 441 | 352 ± 83 | 161 ± 27 |
| HA, vacuum | 6 | 118.5 ± 5 | 274.0 ± 4 | 156 ± 7 | 6316 ± 386 | 393 ± 83 | 156 ± 33 |

The reported uncertainties are one standard deviation of the experimental replicas.

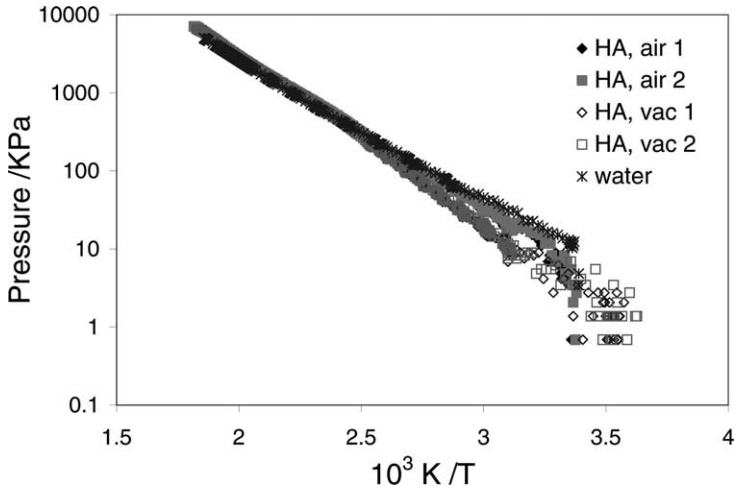


Fig. 2. HA decomposition vapor pressure.

the non-condensable pressure is relatively low (352 kPa (51 psia) in air and 393 kPa (57 psia) in vacuum), which indicates that much of the pressure is due to the vapor pressure of the solvent and products that are liquid at ambient temperature but mainly vapor at $T_{max}$. The vapor pressure of water at $T_{max}$ is approximately 6019 kPa (873 psia), which suggests that much of $\Delta P_{max}$ is due to water and is consistent with the low non-condensable pressure observed. It is important to note that part of the heat produced in the reaction was used to vaporize water, which has a large heat of vaporization. If the reaction were carried out in another solvent with a lower heat of vaporization, the increase in temperature during the reaction should be higher.

Fig. 2 presents the measured vapor pressure curves for the experiments run in the two different environments. This plot is also consistent with the fact that there is relatively little non-condensable pressure produced, since the pressure data are very similar to the vapor pressure of water, and the system can be classified as a hybrid system (the pressure generated during the reaction is produced by both vapor pressure and some non-condensable gas generation) [12].

The non-condensable pressure is a clue to the moles of generated vapor, which can be compared to the theoretical moles of vapor produced by a proposed pathway. Table 3 presents

Table 3
Moles generated and calculated heat released (HR) by HA decomposition

| Sample | Moles of non-condensables generated | $\phi$ factor | HR (kJ/mol) |
|---|---|---|---|
| HA, air | $0.017 \pm 0.004$ | 2.06 | $59 \pm 3$ |
| HA, vacuum | $0.019 \pm 0.004$ | 2.08 | $60 \pm 3$ |

The reported uncertainties are one standard deviation of the experimental replicas.

the moles generated during the reaction calculated as an ideal gas. Assuming Eq. (3), the decomposition of HA in alkaline solutions, the nitrogen gas produced is 0.04 moles, which is approximately twice the observed value. This observation suggests that, even though our samples are alkaline, Eq. (3) is not the only reaction involved in the thermal decomposition of HA during runaway conditions.

Because the APTAC does not directly measure the heat released (HR), the heat of reaction must be estimated. The energy released by the reaction under adiabatic conditions is utilized in three ways: in heating the reaction mass, in vaporizing some of the liquid reaction mixture, and in heating the reaction cell. Table 3 presents estimated heat releases using an average $C_P$ for the sample of 2.80 J/(g °C) (0.669 cal/(g °C)), for which it was assumed that the $C_P$ of the reacting mixture was constant over the entire temperature range. This heat release does not include the heat necessary for evaporating some of the reaction mass, which in this case is significant.

To correct for the evaporation effect, steam tables [13] were used, since approximately 90 mol% of the vapor at $T_{max}$ and a significant portion of the liquid mass is water. This approach, yielding an approximate $\Delta H_{rxn}$ of −117 kJ/mol (−28 kcal/mol), accounts also for some of the non-idealities of the liquid and the gas at high temperatures and pressures. This value is an approximation and includes the following uncertainties: the compositions of the liquid and vapor phases are not known at the initial and final states, some of the heat may be dissipated during the runaway, and some of the sample reacts before the onset temperature. Even though some sample reacts during the heat-wait-search steps below the exotherm, no significant differences in $T_{on}$ or $T_{max}$ were measured when the starting search temperature was 80 °C instead of 50 °C.

When evaluating reaction hazards, we must know not only the amount of heat produced but also how fast this heat is liberated. Fig. 3 shows the measured heat rate with respect to temperature, and Fig. 4 presents the measured pressure rate with respect to temperature. The reproducibility of the experiments can be clearly observed in these graphics. There are no significant differences in these rates between the samples run with air and the samples run in vacuum.

The kinetic equations were presented in [2] and involve guessing a reaction order for a power law reaction rate and linearizing the model. Table 4 presents a summary of the calculated activation energies, frequency factors ($A$), and reaction orders for samples run with air and in vacuum. It is shown that the overall HA decomposition reaction in each environment can be represented with the same reaction order and similar activation energies.

Fig. 5 presents an Arrhenius plot for all experiments assuming an overall reaction order of one. As shown, all experiments have essentially the same Arrhenius plot. Figs. 6 and 7 present the Arrhenius plots for different assumed reaction orders for experiments run with

Table 4
Summary of HA decomposition kinetic parameters

| Sample | Order | $E_a$ (kJ/mol) | $\ln A$ ($\text{min}^{-1}$) |
|---|---|---|---|
| HA, air | 1 | 121 ± 4 | 29.5 ± 1.0 |
| HA, vacuum | 1 | 119 ± 8 | 28.9 ± 2.6 |

The reported uncertainties are one standard deviation of the experimental replicas.

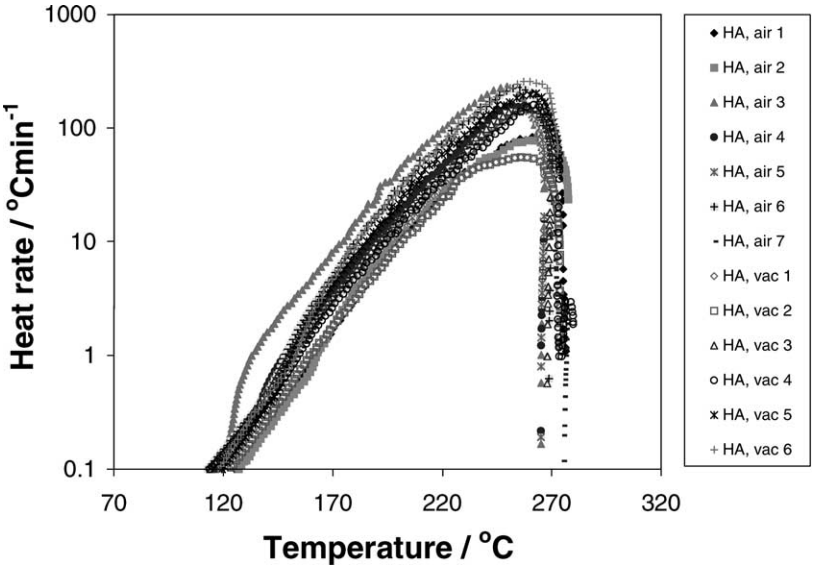


Fig. 3. HA decomposition heat generation.

and without air, respectively. It can be observed from these plots that a good estimate for the overall reaction order is one, because it yields a straight line to validate the model. For comparison, the thermal safety investigation software from *ChemInform* [14] was used to obtain the model parameters by performing a non-linear parameter estimation. The results of both methodologies yielding similar results are shown in Table 5. The overall activation energy is lower than the 61.3 kcal/mol required to break the $H_2N$–OH bond [6], which is the weakest bond of the hydroxylamine molecule.

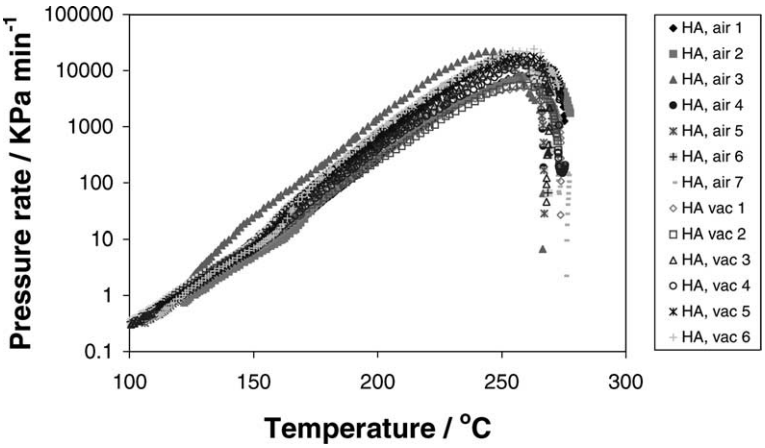


Fig. 4. HA decomposition pressure generation.

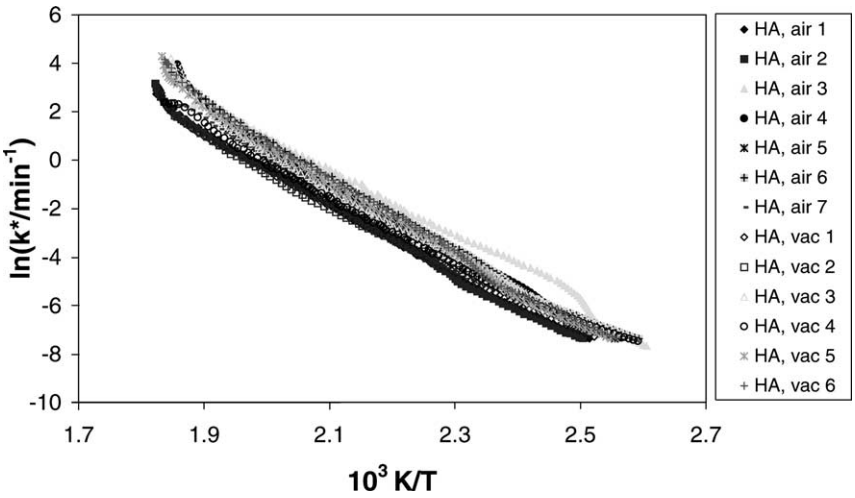


Fig. 5. HA decomposition Arrhenius plot.

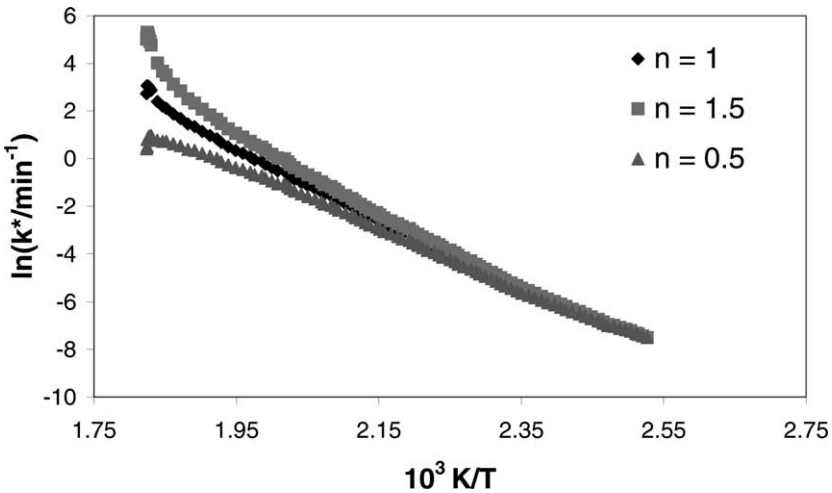


Fig. 6. HA decomposition reaction order in air (99% reaction).

Table 5
HA decomposition kinetic parameters using different methodologies

| Model parameter | Linear parameter estimation | Non-linear parameter estimation |
|---|---|---|
| $E_a$ (kJ/mol) | 121 | 123 |
| $n$ | 1 | 1.08 |
| $\ln A$ ($\text{min}^{-1}$) | 29.5 | 29.7 |

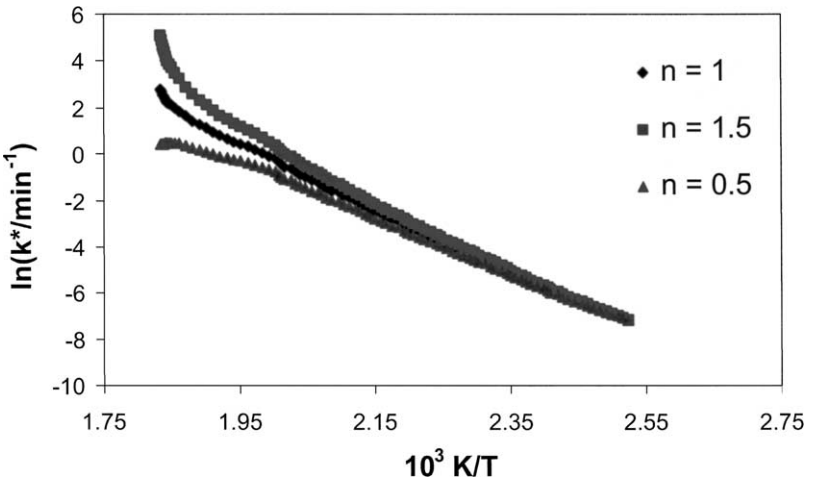


Fig. 7. HA decomposition reaction order in vacuum (99% reaction).

During the experiments, part of the generated heat is absorbed by the sample cell. A common methodology to represent this heat loss is with a $\phi$ factor (ratio of the heat capacity of the sample and the sample cell to the heat capacity of the sample) [2]. The calculated $\phi$ factors for the experiments are presented in Table 3 and were used in the calculation of the heat released. Table 6 presents $T_{on}$, $T_{max}$, and $dT/dt_{max}$ for experiments run in air with different $\phi$ factors. Fig. 8 presents the heat rate versus temperature values for the experiments shown in Table 6, which includes a prediction of heat rate assuming no heat loss to the sample cell ($\phi = 1$) using the methodology described in [12]. As shown in Fig. 8, the predicted $T_{on}$ and $dT/dt_{max}$ for $\phi = 1$ are 115 °C and 53,246 °C/min, respectively. As shown by the considerable increase in the heat rate for the adiabatic system, thermal inertia is an important issue for scaling up of laboratory results to industrial processes, where $\phi$ factors typically are low.

### 4.2. Analytical results

$H_2$ and $N_2$ were detected in the gas sample by GC. Both samples with and without air contained the same chromatographic peaks. EI-FTMS performed in the gas sample showed

Table 6
Parameters at different $\phi$ factors

| $\phi$ | $T_{on}$ (°C) | $T_{max}$ (°C) | $dT/dt_{max}$ (°C/min) |
|---|---|---|---|
| 1.00 | 115[a] | 431[a] | 53246[a] |
| 1.37 | 120 | 282 | 469 |
| 2.00 | 125 | 277 | 83 |
| 3.40 | 136 | 211 | 4 |

[a] Simulated datum.

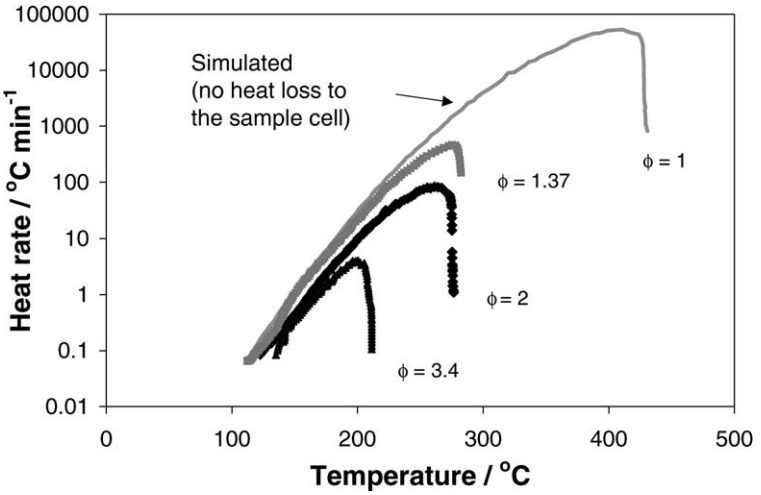


Fig. 8. Effect of thermal inertia on the HA decomposition self-heat rate.

the presence of mainly $N_2$ and $N_2O$ with a small amount of NO. A titration method was used to confirm the presence of ammonia in the final liquid phase (∼8 mass% was detected). The presence of ammonia in the liquid phase was also confirmed by its characteristic odor.

### *4.3. Overall HA decomposition reaction under runaway conditions*

Because no significant difference was observed in the overall HA decomposition reaction run with or without air, it can be assumed that the oxidation path given in Eq. (2) is not significant.

The production of $N_2$ and $N_2O$ during the runaway indicates that both Eqs. (3) and (4) are important during the runaway irrespective of the basic pH of the sample and sample remains. This is expected since during the runaway the increased temperature can activate a wider spectrum of reactions.

## 5. Conclusions

In the thermal decomposition of HA solutions under runaway conditions, $T_{on}$, $T_{max}$, $\Delta P_{max}$, non-condensable pressure, $t_{MR}$, $E_a$, and reaction order are observed not to be significantly affected by the presence of air above the sample. So the detected oxidation products (NO, $N_2O$) are formed primarily by oxygen available within the hydroxylamine molecule. Similar heat rates and pressure rates were measured under air and vacuum conditions. This result shows that an attempt to pacify HA runaway reactions by handling hydroxylamine under oxygen free atmospheres will not result in milder decomposition reactions.

During a HA runaway or process upset, the integrity of glass lined equipment may be compromised since, as shown by our results, glass may dissolve. Another important process

safety related result is that the heat produced by the runaway reaction vaporized a solvent with a large heat of vaporization that tempered the reaction. If hydroxylamine is used in another solvent with a lower heat of vaporization, the temperature and pressure increase should be higher.

The detected gas phase HA decomposition products under runaway conditions for samples run with and without air are $N_2O$, $N_2$, NO, and $H_2$. Ammonia is detected in the liquid residue.

More analytical work is needed to quantify HA decomposition products under runaway conditions, but at present there is no evidence to conclude that these decomposition products will be different for samples with and without air.

## Acknowledgements

We thank Mr. Xianchun Wu of the Chemical Engineering Department at Texas A&M University for the GC measurements and his advice. We express our gratitude to Dr. Robert K. Popp of the Geology and Geophysics Department at Texas A&M University for the semi-quantitative energy disperse spectrum runs. Also, we thank the CONACYT-Fulbright scholarship. This research was sponsored by the Mary Kay O'Connor Process Safety Center at Texas A&M University.

## References

[1] H. Surjono, Z. Xiao, P.C. Sundareswaran, in: Proceedings of the 218th ACS National Meeting, New Orleans, USA, 1999.
[2] L.O. Cisneros, W.J. Rogers, M.S. Mannan, J. Hazard. Mater. 82 (2001) 13.
[3] L.O. Cisneros, W.J. Rogers, M.S. Mannan, in: Proceedings of the Third Annual Mary Kay O'Connor Process Safety Center Symposium on Beyond Regulatory Compliance: Making Safety Second Nature, College Station, TX, 2000, pp. 140–168.
[4] S.M. Kaye, Encyclopedia of Explosives and Related Items, US Army Armament Research and Development Command, Large Caliber Weapon System Laboratory, Springfield, VA; National Technical Information Service, Dover, NY, 1978.
[5] F.R. Bichowsky, F.D. Rossini, Thermochemistry of Chemical Substances, Reinhold, New York, 1936.
[6] R.A. Back, J. Betts, Can. J. Chem. 43 (1965) 2157.
[7] K. Jones, Comprehensive Inorganic Chemistry, Vol. 2, J.C. Bailar, 1973, pp. 265–276.
[8] J.W. Larsen, J. Jandzinski, M. Sidovar, J.L. Stuart, Carbon 39 (2001) 473.
[9] N.I. Kuznetsova, L.I. Kuznetsova, L.G. Detusheva, V.A. Likholobov, G.P. Pez, H. Cheng, J. Mol. Catal. A: Chem. 161 (2000) 1.
[10] S. Lunak, J. Veprek-Siska, Collect. Czechoslov. Chem. Commun. 39 (1974) 391.
[11] S. Chippett, P. Ralbovsky, R. Granville, in: Proceedings of the International Symposium on Runaway Reaction, Pressure Relief Design, and Effluent Handling, 1998, pp. 81–108.
[12] CCPS. Guidelines for Pressure Relief and Effluent Handling Systems, AIChE, New York, NY, 1998.
[13] J.H. Keenan, F.G. Keyes, P.G. Hill, J.G. Moore, Steam Tables, Wiley, New York, NY, 1978.
[14] A. Kossoy, A. Benin, Yu. Akmetshin, in: Proceedings of the Fourth Annual Mary Kay O'Connor Process Safety Center Symposium on Beyond Regulatory Compliance: Making Safety Second Nature, College Station, TX, 2001, pp. 322–336.